High rate lithium intercalation properties of V$_2$O$_5$/carbon/ceramic-filler composites

Shinya Suzuki [a,*], Mitsuhiro Hibino [b], Masaru Miyayama [a]

[a] *Institute of Industrial Science, The University of Tokyo, 4-6-1 Komaba, Meguro-ku, Tokyo 153-8505, Japan*
[b] *National Institute of Advanced Industrial Science and Technology, 1-1-1 Umezono, Tsukuba, Ibaraki 305-8568, Japan*

Abstract

Composite electrodes of amorphous vanadium pentoxide/carbon/ceramic filler were prepared by mixing vanadium oxide hydrosol, acetone, carbon and ceramic fillers, and by extension on aluminum foil. High rate charge/discharge property of the composite electrode was examined, and the effect of fillers was discussed. The composite electrode had a porous structure, in which pores were 0.5–3 μm in diameter and penetrated through the composite. The composite electrode showed a large capacity of 98 mA h/g-electrode at a high current density of 17.2 mA/cm^2 (270 A/g-electrode). The relation between discharge capacity and current density was calculated by solving the simplified diffusion equation. The apparent diffusion coefficient of lithium ion in the composite electrode was found to be 10 times larger than that of electrode without fillers.
© 2003 Elsevier B.V. All rights reserved.

1. Introduction

Electrochemical capacitors with high power density and high energy density capability are attractive energy storage devices for high power applications like electric vehicles and pulsed lasers [1–3], and called "supercapacitors" generally. So far, kinetically fast faradaic processes have been mainly investigated as the high rate electrodes. Surface adsorption to activated carbon [4], insertion of protons into noble metal oxides [5], and p-/n-doping of semiconducting polymers [6] have been studied as the fast faradaic processes applied to the high rate electrodes. Compared with them, supercapacitors using Li$^+$ intercalation reaction into electrode materials, which use another faradaic process, are expected to show both high energy capability and power density.

However, intercalation materials have latent problems to apply to the electrodes of supercapacitors. The diffusion of intercalated ions in the solid phase is rather slow (e.g. the diffusion coefficient of lithium in most intercalation compounds is in the range 10^{-9} to 10^{-13} cm^2/s), and the electronic conductivity of intercalation hosts is usually too low to sustain large currents.

Vanadium pentoxide (V$_2$O$_5$) prepared via sol–gel method is well known as a host for lithium intercalation [7–9]. Electrochemical lithium insertion occurs together with compensating electrons as follows:

$$x\mathrm{Li}^+ + x\mathrm{e}^- + \mathrm{V_2O_5} \rightarrow \mathrm{Li}_x\mathrm{V_2O_5} \tag{1}$$
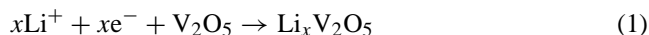
and up to $x = 4$ is said to be able to be incorporated. The capacity is 590 mA h/g(V$_2$O$_5$) when four Li$^+$ per V$_2$O$_5$ are incorporated. The observed diffusion coefficient of lithium insertion is ~10^{-11} cm^2/s [10] at room temperature. To apply V$_2$O$_5$ for the electrodes of supercapacitors, reduction of diffusion length and increase in electronic conductivity are needed. For example, Smyrl and coworkers [11,12] showed an efficiency of composites with nickel felt as a high rate intercalation electrode. Kudo et al. [13] showed that thin layer (<100 nm) V$_2$O$_5$ on carbon particles exhibited a high power density of 190 mA h/g(V$_2$O$_5$) at a high current density of 54 A/g(V$_2$O$_5$).

On the other hand, controlling surface structure of the electrode is another approach for the high rate electrodes. Nanostructured electrodes of V$_2$O$_5$ like the bristles of a brush are reported to be adaptable by Patrissi and Martin [14]. In the present study, microstructure of the V$_2$O$_5$/carbon composite electrode, which is reported by Kudo et al., was modified by ceramic filler to improve lithium diffusion through the electrode.

* Corresponding author. Tel.: +81-3-5452-6464; fax: +81-3-5452-6341.
E-mail address: sin@iis.u-tokyo.ac.jp (S. Suzuki).

2. Experimental

Vanadium pentoxide (V_2O_5) sol was prepared by a reaction of vanadium (Mitsuwa Chemicals, purity 99.5%, ~325 mesh) and hydrogen peroxide (Wako, 30 wt.%) [15]. The V_2O_5 sol, carbon powder (acetylene black, ~70 nm), and ceramic filler were mixed homogeneously with acetone as surfactant. Fibrous tetratitanate, $H_2Ti_4O_9 \cdot 1.9H_2O$ (Otsuka Chemical) with a length of 20 μm and a diameter of 300 nm was used as the filler [16–18]. The electrical conductivity of the fibrous tetratitanate was as small as 10^{-6} S/cm at 130 °C under 0.1 MPa of partial water vapor pressure, therefore the fillers can be treated as insulators. The weight ratio of V_2O_5:carbon:ceramic filler was 1:1.3:3. Composite sheet electrode of V_2O_5/carbon/filler were prepared by extension the mixture on an aluminum foil and drying at 120 °C for 5 h. The morphology of the composite electrodes was characterized by means of a scanning electron microscope and mercury porosimeter. Mass loading of V_2O_5 in the composite electrodes was determined using inductively coupled plasma atomic emission spectrometry, and V_2O_5 amount was 13.7 μg/cm². The average thickness of the composite electrode was 2.0 μm. Electrochemical measurements were performed by using a three-electrode cell with lithium strips as the reference and counter electrodes and composite sheet electrode as the working electrode. The electrolyte solution was 1 M lithium perchlorate in propylene carbonate (Kishida Chemical). Cyclic voltammetry experiments and galvanostatic charge/discharge tests were carried out between the voltage limits of 4.2 and 2.0 V (vs. Li/Li$^+$) with a HAG-5001 (Hokuto Denko) potentiostat/galvanostat. Impedance measurements were conducted by applying 10 mV of a.c. signal amplitude in the frequency range of 20 kHz–100 mHz at 3.0 V (vs. Li/Li$^+$).

3. Results and discussion

Fig. 1(a) and (b) shows scanning electron micrographs of the V_2O_5/carbon/filler composite electrode with different magnifications. The fibers observed are ceramic fillers, and the small particles are V_2O_5/carbon composites. In Fig. 1(a), many pores in size of submicron to a few microns can be observed in the vicinity of fillers, and the pores seem to penetrate through the composite. Since the size of the small particles shown in Fig. 1(b) is similar to that of the carbon particles (~70 nm), the carbon particles are assumed to be covered with a thin layer of V_2O_5, as reported by Kudo et al. [13].

Fig. 2 shows pore size distribution of the V_2O_5/carbon/filler composite (upper part), and the V_2O_5/carbon composite (lower part). Pores of about 0.1 μm are dominant in the composite without fillers (lower), but large pores in the range of 0.5–3 μm exist in the composite with fillers (upper). The pore size of the composite with fillers agrees well with that observed in Fig. 1. It is evident from Figs. 1 and 2 that the
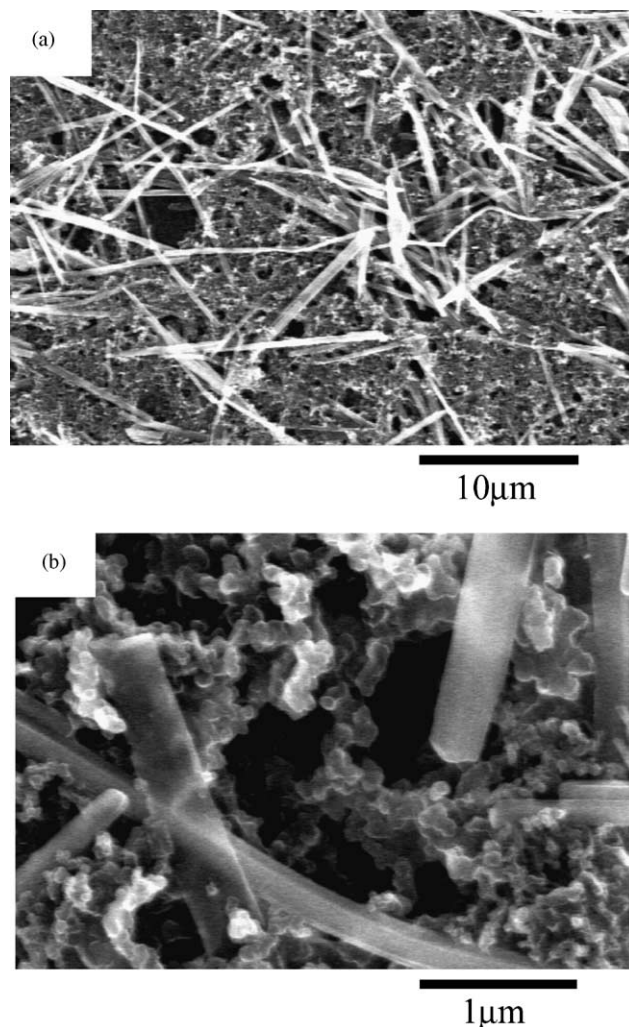

Fig. 1. SEM images of the V_2O_5/carbon/filler composite electrode.

porous structure with large pores is formed by the addition of fillers. This porous structure would be responsible for the permeation of electrolyte within the electrode and the large capacity at high current densities, described later.
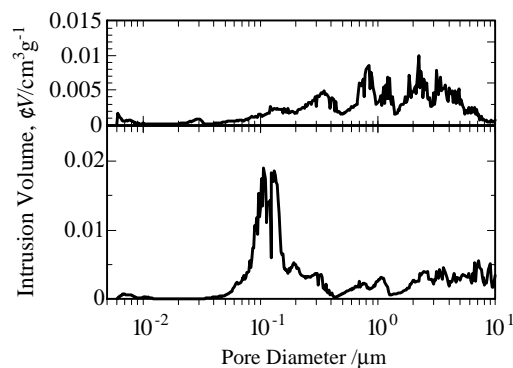

Fig. 2. Comparison of the pore size distribution of the V_2O_5/carbon/filler composites (upper) with the V_2O_5/carbon composites (lower).
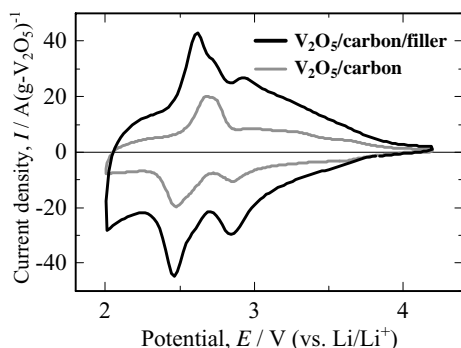
Fig. 3. Cyclic voltammograms for the composite electrodes with and without fillers. The scan rate was 10 mV/s.

Fig. 3 shows cyclic voltammograms for composite electrodes with and without fillers. Two cathodic peaks at 2.5 and 2.8 V were observed. These potentials are same with those observed in V_2O_5 and V_2O_5/carbon electrodes, where the reduction of vanadium occurs [7,11–13,19]. Two anodic peaks were also observed in composite electrode. The anodic peak potential of the composite with filler was a little lower, and the difference between cathodic and anodic peak potentials was less than that without fillers. This would suggest that the charge transfer resistance decreases and then the polarization decreases by mixing fillers.

Fig. 4 shows impedance plots of the composite electrodes with and without fillers at 3.0 V (vs. Li/Li$^+$). The curve of V_2O_5/carbon/filler composite electrode showed a high frequency semicircle and a low frequency straight line, while a high frequency semicircle was followed by an intermediate frequency feature in the curve of V_2O_5/carbon composite electrode. The impedance plot of composite electrode without fillers was similar to that of V_2O_5 aerogel reported by Passerini et al. [12]. They analyzed the impedance behavior and proposed that the high frequency semicircle is
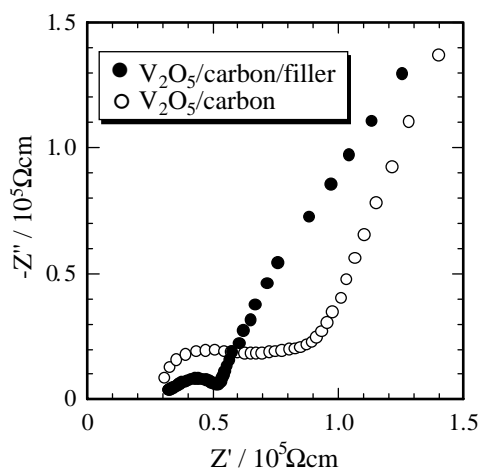

Fig. 4. Impedance plots of the composite electrodes with and without fillers taken in the frequency range of 20 kHz–100 mHz at 3 V (vs. Li/Li$^+$). The a.c. signal amplitude was 10 mV.
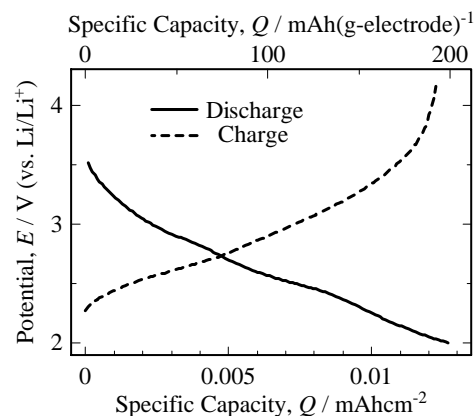

Fig. 5. Discharge and charge curves for V_2O_5/carbon/filler composite electrode at 86 μA/cm^2 (1.35 A/g-electrode). Electrode mass means the sum of V_2O_5, carbon and fillers.

due to the double layer capacitance–electronic resistance of V_2O_5, and the intermediate frequency feature is assigned to the electrode–electrolyte charge transfer process. According to their analysis, it is suggested that the charge transfer resistance was decreased by the addition of fillers in the V_2O_5/carbon/filler composite electrode. The decrease in the charge transfer resistance would be caused by the increase in the interface area between electrode and electrolyte according to the permeation of electrolyte.

Fig. 5 shows discharge and charge curves for V_2O_5/carbon/filler composite electrode measured at the current density of 86 μA/cm^2. Discharge capacity was 12.6 μA h/cm^2 (200 mA h/g-electrode), and this capacity was almost reversible. Discharge curve seems to have two plateaus corresponding to the two cathodic peaks in Fig. 3. Intercalation of Li into the filler material ($H_2Ti_4O_9 \cdot 1.9H_2O$) can be negligible in the measurement voltage region, because the reduction of Ti^{4+} (Ti$^{4+} \rightarrow$ Ti^{3+}) occurs at about 1.6 V (vs. Li/Li$^+$) [20], for example. Consequently, this discharge and charge capacity is caused by V_2O_5. Figs. 3 and 5 show that the capacity of V_2O_5/carbon/filler electrode is exhibited by the reduction and oxidation of vanadium.

Fig. 6 shows discharge curves at various current densities. With increasing current density, the initial ohmic drop increased and the discharge capacity decreased. However, relatively large discharge capacity of 6.2 μA h/cm^2 (98 mA h/g-electrode) still remained at a high current density of 17.2 mA/cm^2 (270 A/g-electrode), which corresponds to the half of discharge capacity at low current density shown in Fig. 5.

Fig. 7 shows discharge capacity as a function of current density in comparison to the V_2O_5/carbon composite electrode without fillers. The V_2O_5/carbon/filler composite electrode showed a larger capacity than that of V_2O_5/carbon composite electrode at every current density. This behavior becomes more striking at higher current densities.

To make clear the reason for the improvement especially at high current densities, difference in lithium diffusion
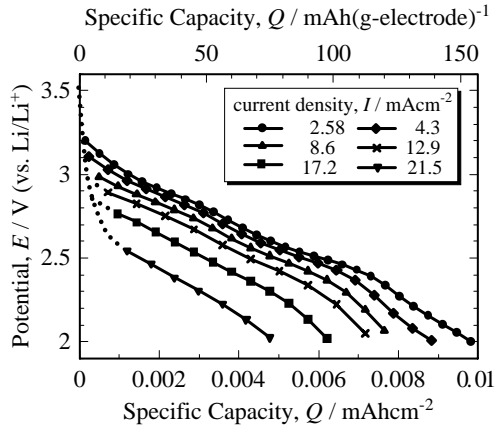
Fig. 6. Discharge curves for V_2O_5/carbon/filler composite electrode at various current densities.

Table 1
Values for estimation of the capacities

Electrode	$\tilde{D}$ ($\times 10^{-10}$ cm^2/s)	Q_0 (mC cm^{-2})	L (μm)
V_2O_5/carbon/filler	92	45.4	2.0
V_2O_5/carbon	9.0	19.1	1.0

behavior between composites with and without fillers is discussed. The following equation (2) can be obtained by solving the one-dimensional diffusion equation under the condition of constant flux at the surface [21]:

$$C - C_0 = \frac{JL}{F\tilde{D}} \left\{ \frac{\tilde{D}t}{L^2} + \frac{1}{3} - \frac{2}{\pi^2} \sum_{n=1}^{\infty} \frac{1}{n^2} \exp\left(-\frac{\tilde{D}n^2\pi^2 t}{L^2} \right) \right\} \tag{2}$$

where C is the lithium concentration, C_0 the initial lithium concentration, J the current density, L the thickness, n a natural number, and $\tilde{D}$ the diffusion coefficient of lithium. When the discharge finishes, the full capacity Q_0 is $LF(C - C_0)$, the discharge capacity Q is Jt. Then the discharge time t is Q_0/J. In this case the discharge capacity Q is described as follows:

$$Q = Q_0 - \frac{JL^2}{3\tilde{D}} + \frac{2JL^2}{\tilde{D}\pi^2} \sum_{n=1}^{\infty} \frac{1}{n^2} \exp\left(-\frac{\tilde{D}n^2\pi^2 Q_0}{L^2 J} \right) \tag{3}$$

According to the above equation, current density dependence of discharge capacity was fitted using $\tilde{D}$ as parameter. Discharge capacity at the current density of 86 μA/cm^2 was applied to Q_0, and an average thickness of the composite to L, respectively. The lines in Fig. 7 show the estimated capacities. Table 1 shows the values used for the estimation.
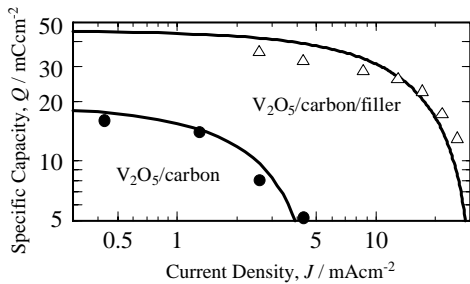
The "apparent" diffusion coefficient of lithium in V_2O_5/carbon/filler composite electrode was 10 times larger than that of electrode without fillers and about 1000 times larger than that of V_2O_5 itself [10,22]. This increase in "apparent" diffusion coefficient would be caused by the porous structure in which electrolyte can permeate into the composite electrode. That is, electrolyte included within the porous electrode will contribute to the increase in "apparent" lithium diffusion coefficient. The full capacity Q_0 of the V_2O_5/carbon/filler electrode was more than twice that of the electrode without fillers. This will be attributed also to the porous structure giving large surface area, enhanced lithium diffusion and consequent complete lithium intercalation into V_2O_5.

The errors in the estimation were relatively large for V_2O_5/carbon/filler composite electrode in Fig. 7. It may be resulted from the inhomogeneous internal structure, which is assumed to be homogeneous in the estimation, in the thickness direction of the V_2O_5/carbon/filler composite electrode or from errors in the measured capacities obtained by cycling measurements.

Fig. 8 shows cycling performance measured between cut-off potentials of 4.2 and 2.5 V (vs. Li/Li$^+$). The second discharge capacity was larger than the first one, but discharge capacity decreased with increasing cycle number after that. After 100 times discharge and charge, the capacity decreased to about half of the initial capacity. The reason for the capacity loss is not clear at present, but the expansion and contraction upon cycling may give physical isolation of V_2O_5 particles each other leading to the capacity loss. Although there is still room for improvement in cycling performance, possibility of the composite electrode for the application to supercapacitors was demonstrated.
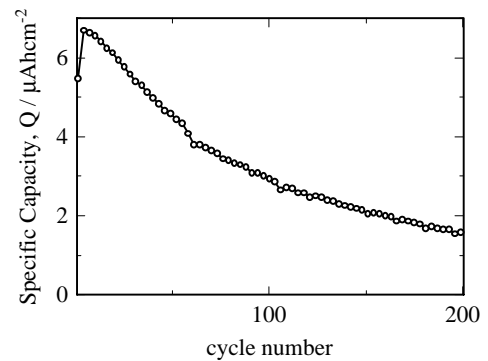

Fig. 7. Discharge capacity of V_2O_5/carbon/filler composite electrode and V_2O_5/carbon composite electrode as a function of current density.

Fig. 8. Cycling performance of V_2O_5/carbon/filler composite electrode. Cycling test was performed at constant current density of 86 μA/cm^2. The cut-off potential was 4.2 and 2.5 V (vs. Li/Li$^+$).

4. Conclusions

Porous V_2O_5/carbon/filler composite electrodes were prepared by mixing ceramic fillers with V_2O_5 sol and carbon particles. The composite electrodes have porous structure in which pores of more than 1 μm penetrate through the composite. The composite electrode showed a capacity of 6.2 μA h/cm^2 (98 mA h/g-electrode) at a high current density of 17.2 mA/cm^2 (270 A/g-electrode). The apparent diffusion coefficient of lithium ion in the composite electrode was 9.2×10^{-9} cm^2/s, and it was 10 times larger than that of electrode without fillers.

Acknowledgements

References

[1] B.E. Conway, Electrochemical Supercapacitors, Kluwer Academic Publishers/Plenum Press, New York, 1999.
[2] A. Rudge, I. Raistrick, S. Gotesfeld, J.P. Ferraris, Electrochim. Acta 39 (1994) 273.
[3] A. Rudge, J. Davey, I. Raistrick, S. Gottesfeld, J.P. Ferraris, J. Power Sources 47 (1994) 89.
[4] D. Galizzioli, F. Tantardini, S. Trasatti, J. Appl. Electrochem. 4 (1974) 57.
[5] B.E. Conway, J. Electrochem. Soc. 138 (1991) 1539.
[6] B.E. Conway, V. Briss, J. Wojtowicz, J. Power Sources 66 (1997) 1.
[7] J. Livage, Chem. Mater. 3 (1991) 578.
[8] K. West, B. Zachau-Christiansen, Jacobson, S. Skaarup, Electrochim. Acta 38 (1993) 1215.
[9] H.K. Park, W.H. Smyrl, M.D. Ward, J. Electrochem. Soc. 142 (1995) 1068.
[10] T. Kudo, M. Hibino, The Electrochemical Society Proceedings, vol. 95, No. 22, Pennington, NJ, USA, 1995, p. 61.
[11] M.J. Parent, S. Passerini, B.B. Owens, W.H. Smyrl, J. Electrochem. Soc. 146 (1999) 1346.
[12] S. Passerini, J.J. Ressler, D.B. Le, B.B. Owens, W.H. Smyrl, Electrochim. Acta 44 (1999) 2209.
[13] T. Kudo, Y. Ikeda, T. Watanabe, M. Hibino, M. Miyayama, H. Abe, K. Kajita, Solid State Ionics 152–153 (2002) 833.
[14] C.J. Patrissi, C.R. Martin, J. Electrochem. Soc. 146 (1999) 3176.
[15] M. Ugaji, M. Hibino, T. Kudo, J. Electrochem. Soc. 142 (1995) 3664.
[16] N. Ohta, Y. Fujiki, Yogyo Kyokaishi 88 (1980) 1.
[17] R. Marchand, L. Brohan, M. Tournoux, Mater. Res. Bull. 15 (1980) 1129.
[18] H. Izawa, S. Kikkawa, M. Koizumi, J. Phys. Chem. 86 (1982) 5023.
[19] M. Giorgetti, S. Passerini, W.H. Smyrl, S. Mukerjee, X.Q. Yang, J. McBreen, J. Electrochem. Soc. 146 (1999) 2387.
[20] S.Y. Huang, L. Kavan, I. Exnar, M. Gratzel, J. Electrochem. Soc. 142 (1995) L142.
[21] J.C. Crank, Mathematics of Diffusion, 2nd ed., Oxford University Press, Oxford, 1975, p. 61.
[22] M. Hibino, T. Kudo, Denki Kagaku 63 (1995) 1040.